Research Article

Lebogang Mogole, Wesley Omwoyo, Elvera Viljoen, and Makwena Moloto*

Green synthesis of silver nanoparticles using aqueous extract of *Citrus sinensis* peels and evaluation of their antibacterial efficacy

https://doi.org/10.1515/gps-2021-0061
received May 28, 2021; accepted September 21, 2021

Abstract: The resistance of microorganisms towards antibiotics remains a big challenge in medicine. Silver nanoparticles (AgNPs) received attention recently for their characteristic nanosized features and their ability to display antimicrobial activities. This work reports the synthesis of AgNPs using the *Citrus sinensis* peels extract in their aqueous, mild, and less hazardous conditions. The effect of concentration variation (1%, 2%, and 3%) of the plant extracts on the size and shape of the AgNPs was investigated. The antimicrobial activities were tested against gram-positive *Staphylococcus aureus* and gram-negative *Klebsiella pneumoniae*. Absorption spectra confirmed the synthesis by the surface Plasmon resonance peaks in the range 400–450 nm for all the AgNPs. FTIR spectra confirmed that *Citrus sinensis* peels extract acted as both reducing and surface passivating agent for the synthesized AgNPs. TEM revealed spherical AgNPs with average size of 12 nm for 3% concentration as compared to the agglomeration at 1% and 2%. All the AgNPs synthesized using *Citrus sinensis* peels extracts (1%, 2%, and 3%) exhibited antimicrobial activity against both gram-positive and negative bacteria. These results indicated a simple, fast, and inexpensive synthesis of silver nanoparticles using the *Citrus sinensis* peels extract that has promising antibacterial activity.

*** Corresponding author: Makwena Moloto,** Institute for Nanotechnology and Water Sustainability, College of Science, Engineering and Technology, University of South Africa, Florida Park, Roodeport, 1709, South Africa, e-mail: Molotmj@unisa.ac.za
Lebogang Mogole, Elvera Viljoen: Department of Biotechnology and Chemistry, Vaal University of Technology, Private Bag X021, Vanderbijlpark, 1900, South Africa
Wesley Omwoyo: Department of Chemistry, Vaal University of Technology, Private Bag X021, Vanderbijlpark, 1900, South Africa; Department of Chemistry, Maasai Mara University, P.O. Box 861-20500, Narok, Kenya

Keywords: surface plasmon resonance, capping agent, antibacterial activity, green synthesis, *Citrus sinensis*

1 Introduction

The resistance of microorganisms towards commonly used antibiotics continues to pose a threat towards the public health. Insufficient sanitation and inadequate medical facilities are among many other factors that cause microorganism such as *Staphylococcus aureus* and *Klebsiella pneumoniae* to become resistant. Some metals in their nanoscale have been reported as promising solutions to overcome the problem of resistant microorganisms and this is due to their high antimicrobial efficiency [1,2].

The science that deals with the preparation of materials in their nanoscale (1–100 nm) is known as nanotechnology [3,4]. Decreasing the size of the material to its nanoscales improves its optical, electrical, and biological properties, thus justifies its use in different fields such as physics, medicine, organic, and inorganic chemistry. Metals such as silver, platinum, and gold in their nanoscale have been reported to have health benefits compared to their bulk material [1,5]. These materials are used in catalysis and sensor technology [6]. Silver nanoparticles, specifically, are extensively applied in many fields due to their unique properties such as thermal, electrical conductivity, and antimicrobial activities [7]. Different methods such as chemical reduction, electrochemical changes, and photochemical reductions can be used to prepare nanoparticles. The selection of the method of preparation of nanoparticles is of importance since factors such as the interaction between the metal ion and the reducing agent as well as the interaction between the nanoparticles and the stabilizing agent have an influence on the size, shape, stability, and the physicochemical properties of the nanoparticles formed [8,9]. Physical methods used to prepare nanoparticles such as milling are not cost-effective since they require high amount of

Open Access. © 2021 Lebogang Mogole *et al.*, published by De Gruyter. This work is licensed under the Creative Commons Attribution 4.0 International License.

energy; furthermore, chemical methods are not eco-friendly since they often require toxic chemicals as starting material and also release toxic or hazardous chemicals, leaving the environment devastated [10]

Green chemistry, on the other hand, focusses on the elimination or minimization of the usage of toxic chemicals. This method is based on the preparation of silver nanoparticles using plants, bacteria, and fungi. The usage of plants when synthesizing silver nanoparticles is considered advantageous since the plants are easily accessible. The method does not require any preparation of culture and any isolation technique. The method is thus considered cost-effective [11,12]. Approximately 140 million of the citrus fruits are produced annually worldwide, thus considered one of the important fruits. *Citrus sinensis*, commonly known as the orange fruit, accounts for about 70% of the produced citrus species. *Citrus sinensis* is often consumed as fresh fruits or used to make orange juice, and after consumption, the peels, which contribute to about 50% of the mass of the fruit, are discarded [13,14].

Orange peels also contain compounds such as phenolic and flavonoids that have been reported to have human health benefits such as antimicrobial and antioxidant activities [15]. The following compounds can also act as potential reducing and capping agents for the synthesis of stabilized silver nanoparticles [16,17]. Hence, the work is reporting on the antimicrobial activity of silver nanoparticles prepared using orange peels.

2 Materials and method

2.1 Chemicals and reagents

Silver nitrate, folin ciocalteu reagent, gallic acid, aluminium chloride, ammonia, quercetin, methanol, sodium carbonate, and sodium hydroxide were all purchased from Sigma Aldrich. Nutrient broth, Muller Hinton Agar, and the bacteria culture were acquired from the Biotechnology laboratories, Vaal University of technology, South Africa.

2.2 Plant extract preparation

The *Citrus sinensis* fruits were purchased from a local supermarket, Pick n Pay stores in South Africa, Gauteng province, Vanderbijlpark, during the 2019 winter season. After peeling the fruits, the *Citrus sinensis* peels were air dried, ground to fine powder using a grinder, and lastly the powder obtained after grinding was passed through the 350 µm sieve. Different concentrations (1%, 2%, and 3%) of the plant extracts were prepared by mixing 1, 2, and 3 g of the *Citrus sinensis* plant with 100 mL double distilled water and allowed to stir for 40 min under constant stirring at 50°C. The mixture was allowed to cool, filtered using the Whattman No 1 filter paper, and centrifuged at 4,000 rpm for 5 min to remove the unwanted material. The supernatant was stored at 4°C until the experiments were conducted.

2.3 Determination of the total phenolic content

The total phenolic content in the *Citrus sinensis* peels was evaluated using the folin ciocalteu assay and gallic acid was used as a standard solution (between 30 and 210 ppm). Briefly, 0.5 mL of the plant extract was mixed with 0.5 mL folin ciocalteu reagent. This was followed by adding 8.5 mL distilled water. UV-Vis spectroscopy was used to measure the absorbance at 725 nm. The concentration of the total phenolic content in the plant extract was calculated from the standard curve ($y = 0.1180x - 0.058$, $r^2 = 0.998$). The total phenolic content was expressed as gallic acid equivalent [18].

2.4 Determination of the total flavonoid content

The total flavonoid in the increasing concentration (1%, 2%, and 3%) in the *Citrus sinensis* was determined using the aluminium chloride method calorimetric method. Briefly 0.5 mL of the extract was mixed with 10% aluminium chloride prepared in methanol and this was followed by addition of 0.1 mL of 1 M potassium acetate. The mixture was allowed to stand for 60 min and the absorbance was measured at 510 nm. Quercetin was used to prepare the calibration curve and the results were expressed as mg quercetin equivalent per g dry weight [19].

2.5 Synthesis of silver nanoparticles

A solution of 0.15 M $AgNO_3$ was prepared in 20 mL ultrapure water. The silver nitrate solution was transferred into a 250 mL three neck flask followed by the addition

of 40 mL *Citrus sinensis* aqueous extract (1%). Ammonia solution was added drop-wise to adjust the pH to 10 to activate the hydroxyl groups. The solution was stirred at room temperature for 2 h, thereafter it was centrifuged at 5,000 rpm for 20 min. The synthesized silver nanoparticles were re-dispersed in methanol and centrifuged to remove impurities. Finally, silver nanoparticles were collected, dried at room temperature, and characterized. Silver nanoparticles capped with 2% and 3% *Citrus sinensis* were synthesized using the same method.

2.6 Characterization

Ultraviolet-visible spectroscopy (Perkin Elmer Lambda 25) was used to study the optical properties of the synthesized silver nanoparticles. Samples were analysed using double distilled water (1 mg·mL^{-1}) transferred into a 1 cm path length cuvettes and scanned from 200 to 1,000 nm. Fourier-transform infrared spectroscopy (Perkin-Elmer Spectrum 400 FT-IR) was used with samples placed on the diamond sample holder and subjected to the infrared radiation measured in the region of 300–4,000 cm^{-1}. JEOL JEM-2100 transmission electron microscope was used to study the morphology of the Ag nanoparticles. Samples were prepared by dispersing the Ag nanoparticles in distilled water, placed on a copper grid, and dried under the infrared lamp. X-ray diffraction (FEI TECNAI SPIRIT) secondary graphite monochromatic Co K alpha radiation (l = 1.7902 Å) was used to study the crystallinity nature of the powdered silver nanoparticles. The scattered radiation was detected in the range $2\theta = 10–60°$ at a scan rate of 2°·min^{-1}.

2.7 Antimicrobial activity: minimum inhibitory concentration (MIC)

The antibacterial activity of the synthesized silver nanoparticles using different concentrations of *Citrus sinensis* (1%, 2%, and 3%) was tested against both gram-positive and gram-negative bacteria, namely *S. aureus* and *K. pneumoniae*, respectively. MIC was carried out to evaluate the lowest concentration of the silver nanoparticles required to prevent visible growth of the microorganisms. Neomycin was used as positive control, while water extract was used as a negative control. Briefly, in this test, a multichannel pipette was used to pour 100 µL of the prepared Mueller Hinton broth into all the wells of the 96 well plate; this was followed by addition of 100 µL of the silver nanoparticles (1 mg·mL^{-1}) into the first row of the 96 well plate. Serial dilution of the silver nanoparticles/neomycin was done by taking 100 µL of the solution in the first row and transferring it into the second row of the plate and taking the 100 µL of the solution in the second row and transferring it into the third row; this dilution was carried out until the last row of the 96 well plate to prepare decreasing concentration solution of the silver nanoparticles. 100 µL of the prepared microbial (*S. aureus*/*K. pneumoniae*) suspension (1×10^6 Cfu·mL^{-1}) was added in all the wells of the 96 well plates. Lastly, 50 µL of the 0.2 mg·mL^{-1} of the *p*-iodonitrotetrazolium chloride (INT) was added also in all the wells of the plate as an indicator. The plates were incubated at 37°C for 24 h and activity was recorded as the blue colouration [16].

2.8 Statistical analysis

Methods 2.3, 2.4, and 2.5 were carried out in triplicates and the representative data are presented here expressed as means ± standard deviation.

3 Results and discussion

3.1 Total phenolic and flavonoid content

The total phenolic and flavonoid contents of *Citrus sinensis* extracts are shown in Figure 1. The total phenolic content ranged from 31 to 78 mg·GAE·mg^{-1} and the flavonoid content ranged between 7 and 32 mg·QAE·mg^{-1}. The highest concentration for both phenols and flavonoids was 3% extract. Thus, the extract can be used both as reducing and stabilizing agent for the synthesis of silver nanoparticles compared to the 1% and 2%. Soto et al. [20] evaluated the total phenolic content in the orange peels extract with total phenolic content of 146.6 GAE per g and similar results were obtained in this study. Jridi et al. [21], furthermore, analysed both the total phenolic and flavonoid content in the dried orange peels extracts with the amounts 8.86 and 6.30 GAE per g, respectively. These results are different to the current study, and this can be attributed to several factors such as the climate, seasons, and geographical conditions of the locations [22].

3.2 UV-Visible spectral analysis

Figure 2 shows the UV-Vis spectra of silver nanoparticles synthesized using the increasing concentration (1%, 2%,

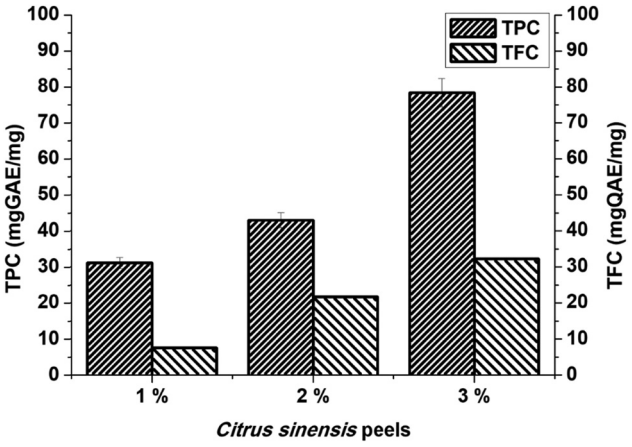

Figure 1: The total phenolic content in different concentrations (1%, 2%, and 3%) of *Citrus sinensis*. Data are mean ± SD (n = 3).

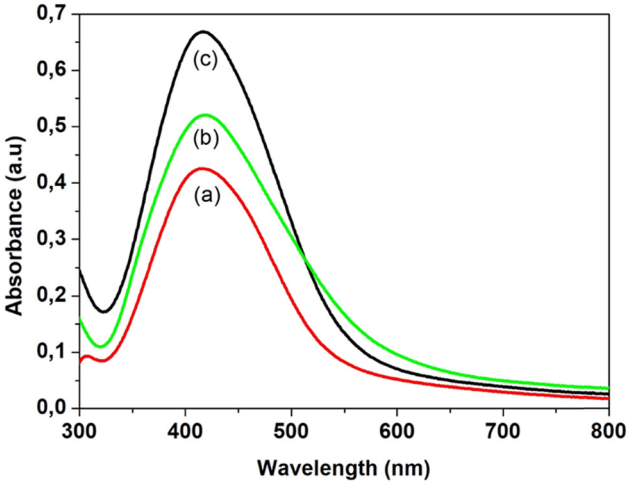

Figure 2: UV-Vis spectra of Ag nanoparticles synthesized using three concentrations of *Citrus sinensis*: (a) 1%, (b) 2%, and (c) 3%.

and 3%) of *Citrus sinensis* extracts. A colour change of yellow to dark brown was observed at pH 10 when both the *Citrus sinensis* and the silver nitrate were mixed. This illustrates successful reduction of Ag^+ ions to produce silver nanoparticles [6].

All the samples showed the surface plasmon resonance (SPR) band which is a characteristic for all noble metals including silver [23]. The SPR peaks for the three concentrations occurred at the same wavelength of approximately 420 nm. The position of the SPR band gives more information about the shape and size of the synthesized silver nanoparticles, and according to the results, the SPR bands shifted to lower wavelengths compared to the bulk material which absorbs at a wavelength of 1,000, thus showing a decrease in particle size [24].

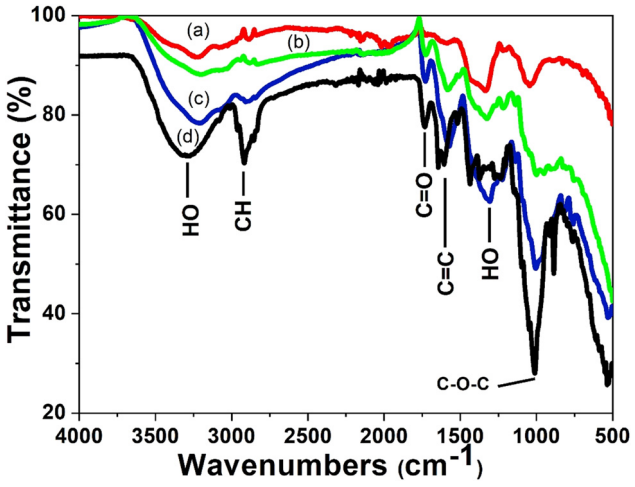

Figure 3: FTIR spectra of the plant extracts and silver nanoparticles synthesized using different concentrations of *Citrus sinensis* peels extract (a) 1%, (b) 2%, (c) 3%, and (d) *Citrus sinensis* peels extract.

3.3 FT-IR spectroscopic analysis

FTIR spectroscopy was also used to confirm the functional groups involved in both the reduction of the silver ion and the stabilization of the silver nanoparticles from the peels. Figure 3 shows the FTIR spectra of the aqueous extract of the *Citrus sinensis* peels and the synthesized nanoparticles using different concentrations of the aqueous extract. Table 1 shows "the summary of FTIR spectral data for the *Citrus sinensis* peels extract and the silver nanoparticles that were synthesized by varying concentration of the extracts". The band at 3,400 cm^{-1} is due to the presence of OH band of the phenolic compounds and carbohydrates; the band at 2,900 cm^{-1} is due to the CH band of the stretching vibration of the aliphatic hydrocarbons chains, either from the methylene or methyl group from the lipids in the aqueous extract. The band at 1,700 cm^{-1} is due to the C═O stretch vibration of the phenolic compounds in the aqueous extracts such as aromatic alkenes. The band at 1,400 cm^{-1} is a characteristic of the aliphatic chains such as the $-CH_2$ and $-CH_3$. The strong peak at 1,010 cm^{-1} is due to the C–O stretching vibration and the band at 900 cm^{-1} is attributed to the OH bonding. The FTIR spectra of the three different concentrations of the *Citrus sinensis* peels extract with nanoparticles were similar to those of the free aqueous extract. However, the OH band in the nanoparticles synthesized using increasing concentration of the extract was found to have shifted to lower frequency with some distortion. This signifies the interaction between the OH group and the Ag^+/Ag^0. The peak at around 1,700 cm^{-1} which can be attributed to C═O was found to increase in intensity as

Table 1: The summary of FTIR spectral data for the *Citrus sinensis* peels extract and the silver nanoparticles that were synthesized by varying concentrations of the extracts

Functional groups	*Citrus sinensis* peels extract wavenumber (cm^{-1})	3% AgNPS-CSP wavenumber (cm^{-1})	2% AgNPS-CSP wavenumber (cm^{-1})	1% AgNPS-CSP wavenumber (cm^{-1})	References
OH	3,311	3,235	3,203	3,202	[4]
CH	2,926	2,919	2,913	2,897	[5]
C═O	1,740	1,732	1,726		[4,6]
C═C	1,648	1,621	1,625	1,611	[7]
–C–H or $–CH_3$	1,440	1,427	1,422	1,415	[8]
C–O–H or C–O–R	1,010	990	1,011	1,066	[9]

the concentration of the extracts was increased from 1% to 3%. This was due to the enhanced availability of the carboxylate group, also shown in Figure 1, where 3% of the extract showed higher phenolic and flavonoid content and 1% showing the least [2]. The results described above suggests that the orange peels extracts contain biomolecules with functional groups such as the O–H and COOH [3]. These functional groups are responsible for the reduction of the Ag^+ to Ag^0; also, they act as stabilizing agents [9]. Scheme 1, given below, shows the proposed mechanism in which the silver ion (Ag^+) interacts with the biomolecules. Briefly, the electron is released from an enol of a phenolic compound. The electron released during the breaking of the H from the –OH bond reduces the Ag^+ to Ag^0 which is the silver nanoparticle. The shift in –OH, which peaks in the FTIR spectra, confirms the proposed mechanism [7].

3.4 Transmission electron microscopic analysis

The morphology of the synthesized nanoparticles was evaluated using the transmission electron microscopy (TEM). TEM images of the silver nanoparticles using the different concentrations of *Citrus sinensis* are presented in Figure 4. According to Figure 4a and b, the synthesized nanoparticles were agglomerated with those synthesized using 1% *Citrus sinensis* peel extract being the most agglomerated. The silver nanoparticles synthesized using 3% *Citrus sinensis* were found to be polydispersed and spherical (Figure 4c), with a particle size distribution from 5 to 25 nm and average diameter of 12 (±10.3) nm. Thus, as the concentration of the *Citrus sinensis* peels increased, the agglomeration decreased. The synthesized nanoparticles in this study were found to have smaller particle size compared to other similar studies [25] of synthesized silver nanoparticles using the *Citrus unshiu*, where the average particle size was found to be 20 nm. Majumdar et al. [26] reported the synthesis of silver nanoparticles using *Citrus macroptera* extract and their observed TEM images displayed particles with an average particle size of 16 (±2.96) nm.

3.5 XRD analysis

XRD spectroscopy was used to study the crystallinity of the synthesized nanoparticles and their structures. Figure 5 shows the XRD patterns of the silver nanoparticles synthesized using the different concentrations of *Citrus sinensis*. According to the Figure 5, four diffraction peaks with 2θ values were observed at 38°, 44°, 64°, and 80°, respectively. The diffraction peaks can be indexed to 111, 200, 220, and 311 planes (JCPDS file No. 04-0788) which confirmed the formation of silver nanoparticles. Samrot et al. [27] and

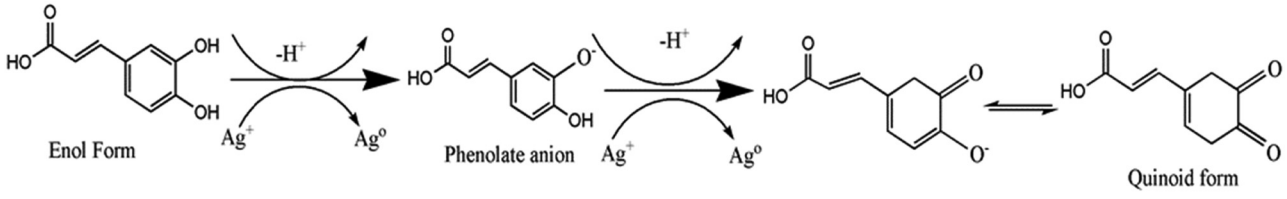

Scheme 1: Proposed mechanism for the synthesis of silver nanoparticles using the extract of *Citrus sinensis* peels.

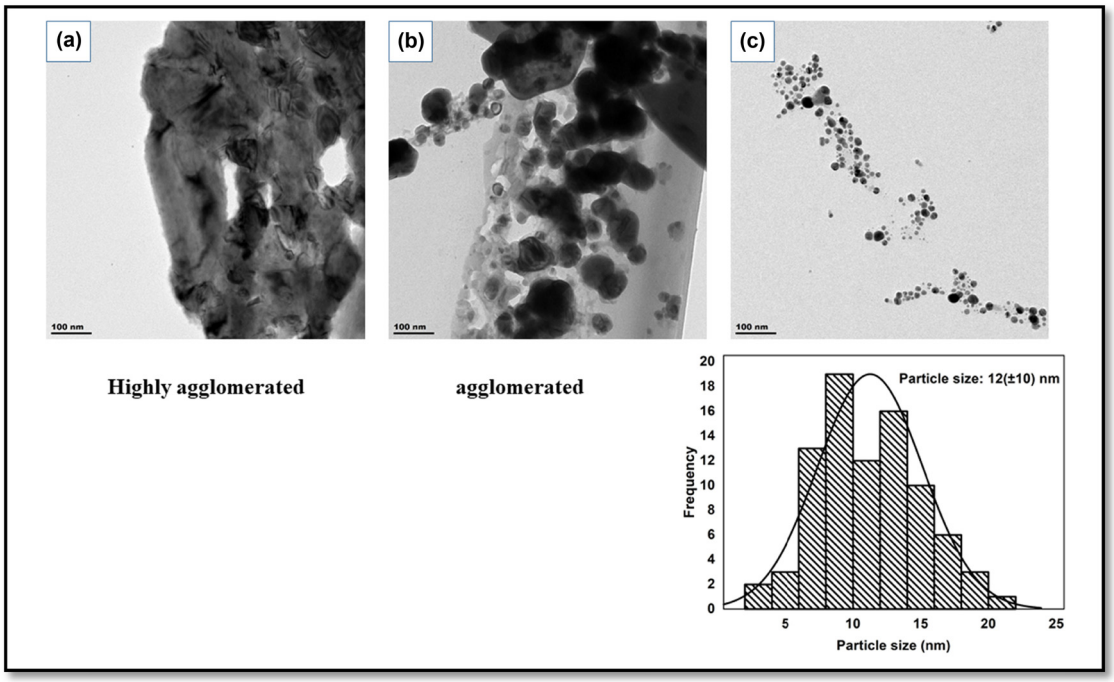

Figure 4: TEM images of silver nanoparticles (a–c) synthesized using different concentrations of *Citrus sinensis* 1%, 2%, and 3%, respectively, and particle size distribution of silver nanoparticles synthesized using 3% *Citrus sinensis*.

Konwarh et al. [28] reported similar characteristic peaks when they synthesized silver nanoparticles using edible fruits and most specifically *Citrus sinensis* peels extracts. The XRD patterns were used to confirm the average particle sizes of silver nanoparticles as 5.3, 5.1, and 4.9 nm for the respective 1%, 2%, and 3% concentrations used. This gave a slight decrease in size as the concentration is increased showing an influence on the extracts used to prepare nanoparticles. The calculated average particle size from the TEM images (Figure 4c) confirmed the presence of small particle size with an average of 5 nm, whereas the lower percentages generally displayed some degree of particle agglomeration.

3.6 Antimicrobial activity of the synthesized nanoparticles

The antimicrobial activity of the synthesized nanoparticles was evaluated using MIC which is defined as the minimum concentration of the sample required to inhibit growth against the tested microorganisms. The synthesized nanoparticles (AgNPs 1%, 2%, and 3%) were tested against gram-negative *K. pneumoniae* and gram-positive *S. aureus*; neomycin was used as a positive control. Table 2 showed the results of antimicrobial activity from the percentages of silver nanoparticles used against the species, *K. pneumoniae* and *S. aureus*. This is due to silver nanoparticles' ability to affect both the chemical and physical properties of the cell walls and cell membranes. This is achieved by the nanoparticles attaching themselves onto the cell which is negatively charged, and as a result, disturbs the important functions such as respiration and osmoregulation [3]. Further on, the synthesized nanoparticles cause damage within the bacteria cell wall by

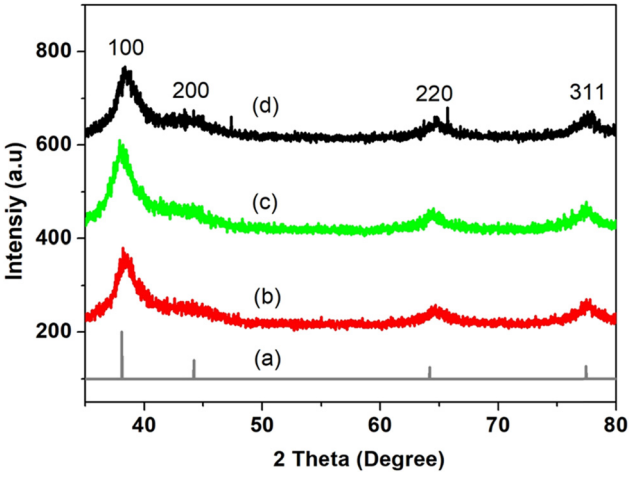

Figure 5: XRD diffraction patterns of silver nanoparticles synthesized using different concentrations of *Citrus sinensis* (a) reference spectrum of silver (b) 1%, (c) 2%, and (d) 3% of AgNPs.

Table 2: Antibacterial activity of silver nanoparticles synthesized using different concentrations of *Citrus sinensis* peels extract

Test organisms	Silver nanoparticles ($mg \cdot mL^{-1}$)			
	1% AgNPs-Cs	2% AgNPs-Cs	3% AgNPs-Cs	Neomycin
Staphylococcus aureus	0.2500	0.2500	0.1250	2.5000
Klebsiella pneumoniae	0.2500	0.1250	0.0625	0.6250

interacting with proteins and DNA after they permeate the bacteria cell wall [29].

The synthesized nanoparticles and the neomycin which was used as a positive control were found to have higher antimicrobial activity against gram-negative *K. pneumoniae* compared to the gram-positive *S. aureus*. Logeswari et al. [7] also reported a similar trend when they synthesized silver nanoparticles using the *Citrus sinensis* peels extracts; their silver nanoparticles gave higher antimicrobial activity against gram-negative *K. pneumoniae* compared to the *S. aureus*. The high activity that was observed against the gram-negative bacteria was attributed to the cell wall. Gram-negative bacteria are known to have thinner walls as compared to the gram-positive bacteria, thus are easier to permeate [30,31]. On the other hand, silver nanoparticles cannot easily permeate and interact with gram-positive bacteria *S. aureus* due to the rigid structure that results from the thick peptidoglycan which consists of peptides cross-linked together giving linear and chains of polysaccharides [32]. The synthesized silver nanoparticles gave better activity compared to the *neomycin* that was used as a positive control. The difference in activity was caused by smaller size and high surface area of silver nanoparticles. Therefore, they have a higher adsorption capacity and thus are more likely to interact with biomolecules [3,10]. According to Table 1 above, 3% Ag nanoparticles gave the lowest MIC values of 0.06250 and 0.1250 $mg \cdot mL^{-1}$ against *K. pneumoniae* and *S. Aureus*, respectively. However, 1% Ag nanoparticles gave 0.2500 $mg \cdot mL^{-1}$ for both the *K. pneumoniae* and *S. aureus*. The high antimicrobial activity that was observed with 3% AgNPs was due to the small size of the silver nanoparticles as shown in the TEM images in Figure 4 compared to the other silver nanoparticles that were synthesized using 1% and 2% AgNPs and were found to be agglomerated [33]. Smaller nanoparticles are known to have high surface area and thus can easily interact with the cell, permeate, and destroy the cell [34]. The reported results by Logeswari et al. [7] obtained particles with an average size of 65 nm from the similar plant species based in a different environment than the peels used in this study. The extracts did not perform as well as compared to species, *S. tricobatum* and *O. tenuiflorum*. These produced highest antimicrobial activity of Ag nanoparticles from the *S. tricobatum* and *O. tenuiflorum* against *S. aureus* (30 mm) and *E. coli* (30 mm), respectively.

4 Conclusion

This study showed green synthesis of silver nanoparticles using increasing concentration of *Citrus sinensis* peels extract (1%, 2%, and 3%). The *Citrus sinensis* peels were found to contain significant amount of phenols and flavonoid content, which are phyto-constituents that are responsible for the reduction of Ag^{1+} to Ag^{0} and for capping and stabilizing silver nanoparticles. XRD indicated that the average crystallite sizes (about 5 nm) showed an insignificant decrease of 0.2 nm as the concentration of the peels extracts increased from 1% to 3%. The *Citrus sinensis* extract concentrations did not influence the crystallite size. UV-Vis spectroscopy showed that the synthesized AgNPs exhibited a surface Plasmon resonance which is a characteristic peak for AgNPs particles. FTIR showed the presence of biomolecules that might be responsible for the reduction of the silver ion and stabilizing of the silver nanoparticles during the synthesis of AgNPs. TEM showed that 3% *Citrus sinensis* gave non-agglomerated spherical-shaped silver nanoparticles with an average size of 12 nm and further showed that, as the concentration of the *Citrus sinensis* decreased from 3% to 1%, the particles became more agglomerated. All the synthesized AgNPs showed antimicrobial activity against both gram-positive and gram-negative bacteria. The synthesized AgNPs can be used as a potential antimicrobial agent even at lower concentration of extracts.

Funding information: This work was supported financially by the National Research Foundation (NRF) South Africa grant No: 120863.

Author contributions: Lebogang Mogole: writing – original draft, data – collection, writing – review and editing, methodology, formal analysis; Wesley Omwoyo: writing – original draft, formal analysis, assisted in project administration; Elvera Viljoen: provided support for the XRD

analysis and reviewed the manuscript, purchased some of the reagents; Makwena Moloto: principal researcher, formulation of the research concept, provided budget and resources for research, assisted in data interpretation, reviewed the manuscript.

Conflict of interest: Authors state no conflict of interest.

Data availability statement: All the necessary data have been provided in the manuscript, but any extra or additional information can be made available upon request.

References

[1] Magiorakos A, Srinivasan A, Carey RB, Carmeli Y, Falagas ME, Giske CG, et al. Multidrug-resistant, extensively drug-resistant and pandrug-resistant bacteria: an international expert proposal for interim standard definitions for acquired resistance. Clin Microbiol Infect. 2012;18(3):268–81.

[2] Panáček A, Kvítek L, Smékalová M, Večeřová R, Kolář M, Röderová M, et al. Bacterial resistance to silver nanoparticles and how to overcome it. Nat Nanotechnol. 2018;13:65–71.

[3] Sharma VK, Yngard RA, Lin Y. Silver nanoparticles: green synthesis and their antimicrobial activities. Adv Colloid Interface Sci. 2009;145(1–2):83–96.

[4] Yan-yu Ren, Hui Yang, Tao Wang, Chuang Wang. Green synthesis and antimicrobial activity of monodisperse silver nanoparticles synthesized using Ginkgo Biloba leaf extract. Phys Lett A. 2016;380(45):3773–7.

[5] Govindrao P, Ghule NW, Haque A, Kalaskar MG. Journal of drug delivery science and technology metal nanoparticles synthesis : an overview on methods of preparation, advantages and disadvantages, and applications. J Drug Delivery Sci Technol. 2018;53:101174.

[6] Thomas B, Mary S, Vithiya B, Arul TA. Science direct antioxidant and photo catalytic activity of aqueous leaf extract mediated green synthesis of silver nanoparticles using passiflora edulis F. flavicarpa. Mater Today: Proc. 2019;14:239–47.

[7] Logeswari P, Silambarasan S, Abraham J. Synthesis of silver nanoparticles using plants extract and analysis of their antimicrobial property. J Saudi Chem Soc. 2015;19(3):311–7. doi: 10.1016/j.jscs.2012.04.007.

[8] Barberia-roque L, Gámez-espinosa E, Viera M, Bellotti N. International biodeterioration & biodegradation assessment of three plant extracts to obtain silver nanoparticles as alternative additives to control biodeterioration of coatings. Int Biodeterior Biodegrad. 2017;141:52–61.

[9] Ibrahim HMM. Green synthesis and characterization of silver nanoparticles using banana peel extract and their antimicrobial activity against representative microorganisms. J Radiat Res Appl Sci. 2015;8(3):265–75.

[10] Ren Y, Yang H, Wang T, Wang C. Bio-synthesis of silver nanoparticles with antibacterial activity. Mater Chem Phys. 2019;235:121746–84.

[11] Bar H, Bhui DK, Sahoo GP, Sarkar P, De SP, Misra A. Aspects green synthesis of silver nanoparticles using latex of jatropha curcas, colloids and surfaces a: physicochemical and engineering. 2009;339:134–9.

[12] Ruíz-baltazar ÁDJ, Maya-cornejo J, Rodríguez-morales AL, Esparza R. Results in physics alcoholic extracts from paulownia tomentosa leaves for silver nanoparticles synthesis. Results Phys. 2018;12:1670–9.

[13] Abbate L, Tusa N, Fatta S, Bosco D, Strano T, Renda A, et al. Genetic improvement of Citrus fruits: new somatic hybrids from Citrus sinensis (L.) Osb. and Citrus limon (L.) Burm. F. FRIN. 2012;48(1):284–90.

[14] Balasundram N, Sundram K, Samman S. Phenolic compounds in plants and agri-industrial by-products: Antioxidant activity, occurrence, and potential uses. Food Chem. 2006;99(1):191–203.

[15] Gorinstein S, Martín-Belloso O, Park YS, Haruenkit R, Lojek A, Číž M, et al. Comparison of some biochemical characteristics of different citrus fruits. Food Chem. 2001;74(3):309–15.

[16] Behravan M, Hossein A, Naghizadeh A, Ziaee M, Mahdavi R, Mirzapour A. International journal of biological macromolecules facile green synthesis of silver nanoparticles using berberis vulgaris leaf and root aqueous extract and its antibacterial activity. Int J Biol Macromolecules. 2019;124:148–54.

[17] Tripathi D, Modi A, Narayan G, Pandey S. Materials science & engineering C green and cost effective synthesis of silver nanoparticles from endangered medicinal plant Withania coagulans and their potential biomedical properties. Mater Sci & Eng C. 2017;100:152–64.

[18] Cappellari L, del R, Santoro MV, Nievas F, Giordano W, Banchio E. Increase of secondary metabolite content in marigold by inoculation with plant growth-promoting rhizobacteria. Appl Soil Ecol. 2013;70:16–22.

[19] Khaleghnezhad V, Yousefi AR, Tavakoli A, Farajmand B. Interactive effects of abscisic acid and temperature on rosmarinic acid, total phenolic compounds, anthocyanin, carotenoid and flavonoid content of dragonhead (Dracocephalum moldavica L.). Sci Horticulturae. 2018;250:302–9.

[20] Soto KM, Quezada-Cervantes CT, Hernández-Iturriaga M, Luna-Bárcenas G, Vazquez-Duhalt R, Mendoza S. Fruit peels waste for the green synthesis of silver nanoparticles with antimicrobial activity against foodborne pathogens. LWT. 2019;103:293–300.

[21] Jridi M, Boughriba S, Abdelhedi O, Nciri H, Nasri R, Kchaou H, et al. Investigation of physicochemical and antioxidant properties of gelatin edible film mixed with blood orange (Citrus sinensis) peel extract. Food Packaging Shelf Life. 2019;21:100342.

[22] Ahmed AF, Attia FAK, Liu Z, Li C, Wei J, Kang W. Antioxidant activity and total phenolic content of essential oils and extracts of sweet basil (Ocimum basilicum L.) plants. Food Sci Hum Wellness. 2019;8(3):299–305.

[23] Bindhu MR, Umadevi M. Synthesis of monodispersed silver nanoparticles using Hibiscus cannabinus leaf extract and its antimicrobial activity. Spectrochim Acta - Part A: Mol Biomol Spectrosc. 2013;101:184–90.

[24] Chahar V, Sharma B, Shukla G, Srivastava A, Bhatnagar A. Study of antimicrobial activity of silver nanoparticles synthesized using green and chemical approach. Colloids Surf A. 2018;554:149–55.

[25] Basavegowda N, Rok Lee Y. Synthesis of silver nanoparticles using Satsuma mandarin (Citrus unshiu) peel extract: A novel approach towards waste utilization. Mater Lett. 2013;109:31–3.
[26] Majumdar M, Khan SA, Biswas SC, Roy DN, Panja AS, Misra TK. In vitro and in silico investigation of anti-biofilm activity of Citrus macroptera fruit extract mediated silver nanoparticles. J Mol Liq. 2020;302:112586.
[27] Samrot AV, Raji P, Jenifer Selvarani A, Nishanthini P. Antibacterial activity of some edible fruits and its green synthesized silver nanoparticles against uropathogen – Pseudomonas aeruginosa SU 18. Biocatal Agric Biotechnol. 2018;16:253–70.
[28] Konwarh R, Karak N, Sarwan EC, Baruah S, Mandal M. Effect of sonication and aging on the templating attribute of starch for "green" silver nanoparticles and their interactions at bio-interface. Carbohydr Polym. 2011;83(3):1245–52.
[29] Ahn E, Jin H, Park Y. Assessing the antioxidant, cytotoxic, apoptotic and wound healing properties of silver nanoparticles green-synthesized by plant extracts. Mater Sci Eng C. 2018;101:204–16.
[30] Dakshayani SS, Marulasiddeshwara MB, Kumar MNS, Ramesh G, Kumar PR, Devaraja S, et al. Antimicrobial, anti-coagulant and antiplatelet activities of green synthesized silver nanoparticles using Selaginella (Sanjeevini) plant extract. Int J Biol Macromol. 2019;131:787–97.
[31] Vigneshwaran N, Ashtaputre NM, Varadarajan PV, Nachane RP, Paralikar KM, Balasubramanya RH. Biological synthesis of silver nanoparticles using the fungus Aspergillus flavus. Mater Lett. 2007;61(6):1413–8.
[32] Rashid S, Azeem M, Ali S, Maroof M. Biointerfaces characterization and synergistic antibacterial potential of green synthesized silver nanoparticles using aqueous root extracts of important medicinal plants of Pakistan. Colloids Surf B. 2018;179:317–25.
[33] Hernández-morales L, Espinoza-gómez H, Flores-lópez LZ, Sotelo-barrera EL, Núñez-rivera A, Cadena-nava RD, et al. Study of the green synthesis of silver nanoparticles using a natural extract of dark or white Salvia hispanica L seeds and their antibacterial application. Appl Surf Sci. 2019;489:952–61.
[34] Jemilugba OT, Hadji E, Sakho M, Parani S. Green synthesis of silver nanoparticles using Combretum erythrophyllum leaves and its antibacterial activities. Colloid Interface Sci Commun. 2019;31:100191.